

## Electron-energy-loss studies of $\text{Rb}_x\text{C}_{60}$ and $\text{Rb}_x\text{C}_{70}$ ( $x = 0, 3,$ and $6$ )

E. Sohmen and J. Fink

*Kernforschungszentrum Karlsruhe, Institut für Nukleare Festkörperphysik,  
Postfach 3640, W-7500 Karlsruhe, Federal Republic of Germany*

(Received 30 November 1992)

The electronic structure of undoped and Rb-doped  $\text{C}_{60}$  and  $\text{C}_{70}$  has been studied by high-energy electron-energy-loss spectroscopy in transmission. Excitations of valence and core electrons reveal the occupation of bands derived from the lowest unoccupied molecular orbitals upon  $n$ -type doping of the solid fullerenes. Detailed information on the electronic structure of  $\pi$  and  $\sigma$  electrons is provided.

### I. INTRODUCTION

The discovery of fullerene molecules<sup>1</sup> and the synthesis of macroscopic amounts of fullerenes<sup>2</sup> has allowed the preparation of a class of solids with interesting properties. In particular, the  $\text{C}_{60}$ -based salts (fullerides),  $A_x\text{C}_{60}$  ( $A = \text{K}, \text{Rb},$  and  $\text{Cs}$ ) and similar compounds with mixtures of alkali metals form synthetic metals for  $x = 3$ , with conductivities of up to  $\sigma \sim 500$  S/cm (Ref. 3) and show superconductivity<sup>4</sup> with remarkably high transition temperatures,  $T_c$ , of up to 33 K.<sup>5</sup> In the analogous compounds of  $\text{C}_{70}$ , the observed conductivities are reduced by two orders of magnitude<sup>3</sup> and to our knowledge no superconductivity has been detected in these materials.<sup>6</sup> The mechanism of superconductivity in the  $\text{C}_{60}$  compounds is not clear. Currently, it is under discussion whether coupling of the conduction electrons to molecular vibrations<sup>7-9</sup> or to low-energy phonons<sup>10</sup> or whether electron-correlation based couplings<sup>11</sup> are operative. A prerequisite for the resolution of the mechanism for superconductivity in these compounds is the understanding of the electronic structure in the normal state. There have been several high-energy spectroscopic studies of the electronic structure of solid fullerenes (fullerites) and fullerides by photoemission,<sup>12-17</sup> inverse photoemission,<sup>13,16</sup> x-ray-absorption spectroscopy,<sup>14,18</sup> and high-energy electron-energy-loss spectroscopy (EELS).<sup>19,20</sup> In addition, we mention investigations of the electronic structure of fullerites and fullerides by optical spectroscopy<sup>21-26</sup> and by low-energy electron-energy-loss spectroscopy.<sup>27,28</sup> From the theoretical side there have been numerous investigations of the electronic structure by band-structure calculations.<sup>29-32</sup> Optical properties of fullerites and alkali-metal-based fullerides have been calculated by several groups.<sup>33-35</sup>

The picture of the electronic structure that emerges from experiment and theoretical calculations is dominated by molecular orbitals. Strong  $\sigma$  bonds in the surface of the  $\text{C}_{60}$  molecule form the cage. In addition, there are less strongly bonded  $\pi$  orbitals perpendicular to the surface. The molecular properties can be easily understood by tight-binding calculations. In the solid, narrow  $\pi$  bands are formed which determine the transport properties of doped fullerenes. A great deal of the solid-state electronic structure can be explained by band-structure

calculations in the local-density approximation. Stimulated by photoemission, inverse photoemission, and Auger-spectroscopy measurements<sup>36</sup> and by theoretical estimates,<sup>37</sup> there is now a lively debate as to whether correlation effects are important in these systems or whether the electronic structure can be adequately described in a one-electron picture.

In this contribution we have studied the electronic structure of  $\text{Rb}_x\text{C}_{60}$  and  $\text{Rb}_x\text{C}_{70}$  ( $x = 0, 3,$  and  $6$ ). Part of the results have been published previously.<sup>38</sup> From x-ray diffraction we know that at room temperature  $\text{C}_{60}$  and  $\text{Rb}_3\text{C}_{60}$  has an fcc structure, while  $\text{Rb}_6\text{C}_{60}$  has a bcc structure.<sup>39-43</sup> Under special preparation conditions, a  $\text{Rb}_4\text{C}_{60}$  phase has also been observed.<sup>41</sup> To the best of our knowledge, no structural investigations on  $\text{Rb}_x\text{C}_{70}$  have been published. The undoped  $\text{C}_{60}$  and the fully doped  $\text{Rb}_6\text{C}_{60}$  are insulating compounds, while  $\text{Rb}_3\text{C}_{60}$  is metallic with a room-temperature conductivity of 100 S/cm.<sup>3</sup> From a comparison of conductivity measurements of  $\text{K}_x\text{C}_{60}$  and  $\text{K}_x\text{C}_{70}$ , we also expect  $\text{C}_{70}$  and  $\text{Rb}_6\text{C}_{70}$  to be an insulator and  $\text{Rb}_3\text{C}_{70}$  to be a "metal" with a conductivity below 1 S/cm.<sup>3</sup> Superconductivity has been observed below  $T_c = 28$  K for  $\text{Rb}_3\text{C}_{60}$ ,<sup>44</sup> but not for  $\text{Rb}_3\text{C}_{70}$ .

The investigations of the electronic structure of the fullerides presented here have been performed by electron-energy-loss spectroscopy (EELS) in transmission. We emphasize that this technique is not surface sensitive, unlike most of the other high-energy spectroscopies (e.g., photoemission). Low-energy data ( $E < 40$  eV) provide information on collective excitations and interband transitions related to  $\pi$  and  $\sigma$  bands. Dielectric functions over a wide energy range have been derived for all compounds  $\text{Rb}_x\text{C}_{60}$  and  $\text{Rb}_x\text{C}_{70}$  ( $x = 0, 3,$  and  $6$ ). Core-level excitations at higher energies measure in a first approximation the local density of unoccupied states at the excited atom.

### II. EXPERIMENT

The fullerenes  $\text{C}_{60}$  and  $\text{C}_{70}$  were prepared by the contact-arc method following Krätschmer *et al.*,<sup>2</sup> with subsequent extraction with toluene. Separated  $\text{C}_{60}$  and  $\text{C}_{70}$  were obtained using liquid phase chromatography with a hexane-toluene solution on alumina. Films with a thickness of 500–2000 Å were prepared by evaporation of the fullerenes at  $\sim 550^\circ\text{C}$  from a Knudsen cell under

high-vacuum conditions onto NaCl single crystals. The NaCl substrate was then dissolved in water and the films were floated onto standard electron microscopy grids. To remove contamination from solvents, oxygen, or water, the films were heated in the EELS spectrometer to  $300^\circ\text{C}$  for 20 min under ultrahigh vacuum (UHV) conditions.

For doping with Rb, various amounts of Rb metal were evaporated onto the fullerene films from commercial SAES Getters sources (SAES Getters, Milano, Italy), while maintaining chamber pressures below  $1 \times 10^9$  Torr. During doping the samples were heated to  $\sim 150^\circ\text{C}$  to improve homogeneity. The films were then transferred under UHV conditions to the EELS spectrometer.

The Rb concentrations in  $\text{Rb}_x\text{C}_{60}$  were determined by comparing electron-diffraction data, taken with the EELS spectrometer setting the energy loss to zero, with x-ray-diffraction data on  $\text{Rb}_x\text{C}_{60}$  from the literature.<sup>43</sup> Typical electron-diffraction data from  $\text{Rb}_x\text{C}_{60}$  for  $x = 0, 3,$  and  $6$  are shown in Fig. 1. We estimate that the accuracy of the quoted Rb concentration for  $x = 3$  is about 5%. For  $\text{Rb}_x\text{C}_{70}$  the determination of the Rb concentration is more difficult. The fully doped  $\text{C}_{70}$  was assigned to the composition  $\text{Rb}_6\text{C}_{70}$ . From the various samples having intermediate Rb concentrations, the one which had diffraction data (see Fig. 1) closest to  $\text{Rb}_3\text{C}_{60}$  and which

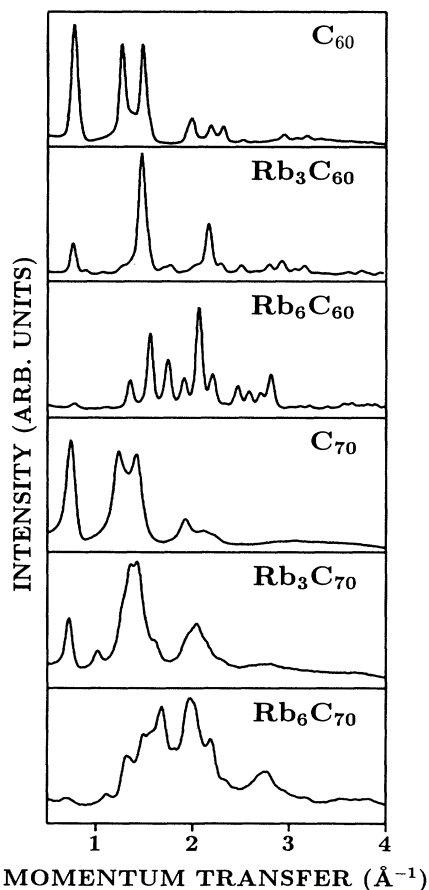


FIG. 1. Electron-diffraction data on typical  $\text{Rb}_x\text{C}_{60}$  and  $\text{Rb}_x\text{C}_{70}$  samples for  $x = 0, 3,$  and  $6$ .

had the highest spectral weight in the loss function below  $\sim 1$  eV was assigned to  $\text{Rb}_3\text{C}_{70}$ . At the spectrometer pressure of  $\sim 2 \times 10^{-10}$  Torr the samples were found to be stable for several weeks. Both EELS spectra and electron-diffraction data were recorded in transmission with a spectrometer<sup>45</sup> having a primary beam energy of 170 keV. The energy resolution of the spectrometer was set to 0.14 eV. The momentum resolution was chosen  $0.04 \text{ \AA}^{-1}$  for valence-band excitations and elastic scattering, while it was set to  $0.20 \text{ \AA}^{-1}$  for core-level excitations.

### III. RESULTS

In Fig. 2 we show the loss functions,  $\text{Im}(-1/\epsilon)$ , for  $\text{C}_{60}$ ,  $\text{Rb}_3\text{C}_{60}$ , and  $\text{Rb}_6\text{C}_{60}$  as derived from the energy-loss spectra taken at a momentum transfer of  $q = 0.15 \text{ \AA}^{-1}$ . Similar data are shown in Fig. 3 for  $\text{C}_{70}$ ,  $\text{Rb}_3\text{C}_{70}$ , and  $\text{Rb}_6\text{C}_{70}$ . The contributions of quasielastic scattering at zero energy and contributions due to multiple scattering<sup>46</sup> have been removed. In addition, the spectra must be corrected for kinematic effects which arise from the energy dependence of the  $1/q^2$  weighting factor appearing in the formula for the cross section for inelastic electron scattering. In order to obtain the absolute value of the loss functions, a Kramers-Kronig analysis has been performed. In the cases where the optical refractive index  $n$  at small energies ( $E < 1$  eV) is known, the final scale of the loss function has been derived from the condition

$$\text{Re}[-1/\epsilon(0,0)] = -1/\epsilon_1(0,0) = -1/n^2.$$

For solid  $\text{C}_{60}$  and  $\text{C}_{70}$  refractive indices of  $n \sim 2$  have been reported.<sup>22,25</sup> For compounds with Rb concentrations corresponding to  $x = 3$  and  $6$ , the oscillator strength sum rule assuming  $N_{\text{eff}}(\omega \gg \omega_p) = 4n_c$  electrons ( $n_c = \text{number}$

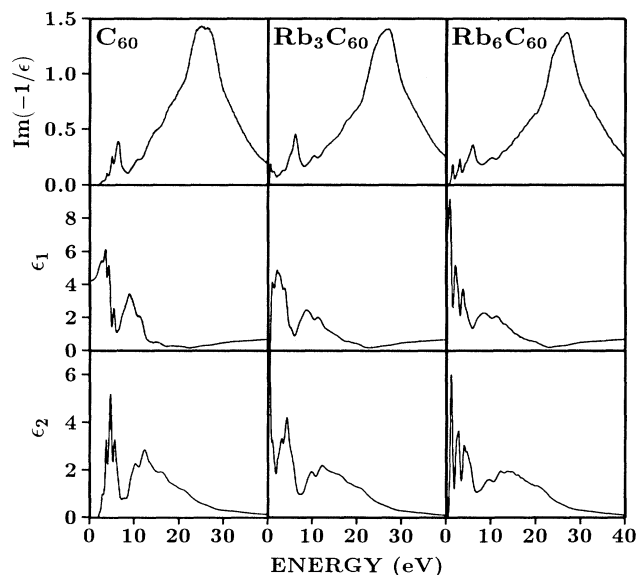


FIG. 2. Electron-energy-loss function,  $\text{Im}(-1/\epsilon)$ , real part of the dielectric function,  $\epsilon_1$ , and imaginary part of the dielectric function,  $\epsilon_2$ , for  $\text{Rb}_x\text{C}_{60}$  ( $x = 0, 3,$  and  $6$ ). The momentum transfer is  $q = 0.15 \text{ \AA}^{-1}$ .

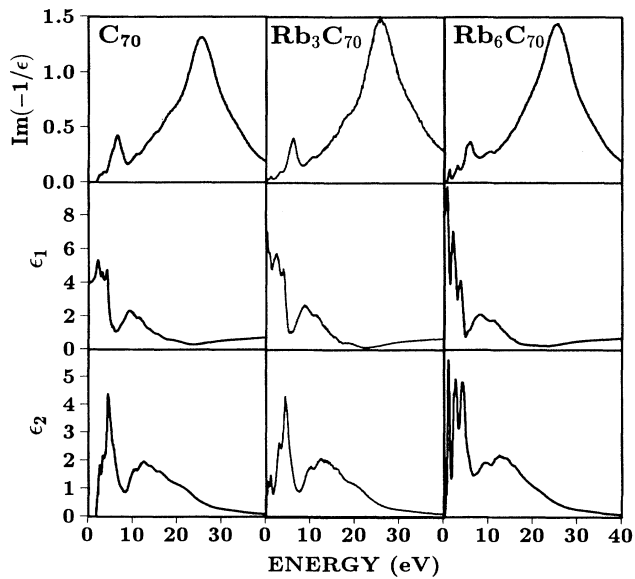


FIG. 3. The same as in Fig. 2 but for  $\text{Rb}_x\text{C}_{70}$  ( $x=0, 3,$  and  $6$ ).

of carbon atoms per molecule) has been used to calibrate the absolute value of the loss function. The contributions due to valence electrons and shallow core-level electrons of the Rb atoms slightly enhance  $N_{\text{eff}}$ .

As discussed in our previous EELS studies on solid  $\text{C}_{60}$  and  $\text{C}_{70}$ ,<sup>19</sup> the loss functions of undoped and alkali-metal-doped fullerenes show a prominent feature at about 26 eV which can be ascribed to a plasmon of all valence electrons stemming from  $\pi+\sigma$  electrons of the fullerene molecules and in the doped materials also from the Rb5s and Rb4p electrons. Below  $\sim 8$  eV there are several " $\pi$  plasmons" caused by  $\pi\rightarrow\pi^*$  interband transitions. Above  $\sim 8$  eV several shoulders on the  $\pi+\sigma$  plasmon are observed which are caused by  $\sigma\rightarrow\sigma^*$  and mixed  $\pi\rightarrow\sigma^*$  or  $\sigma\rightarrow\pi^*$  interband transitions.

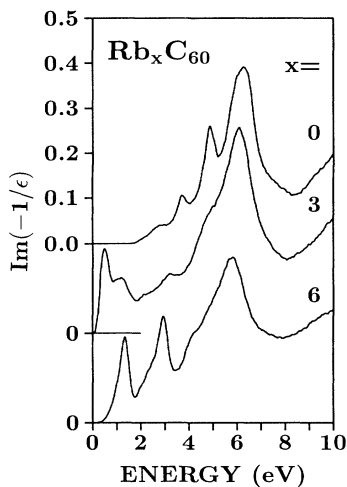


FIG. 4. Low-energy-loss function of  $\text{Rb}_x\text{C}_{60}$  for  $x=0, 3,$  and  $6$ . The momentum transfer is  $q=0.15 \text{ \AA}^{-1}$ .

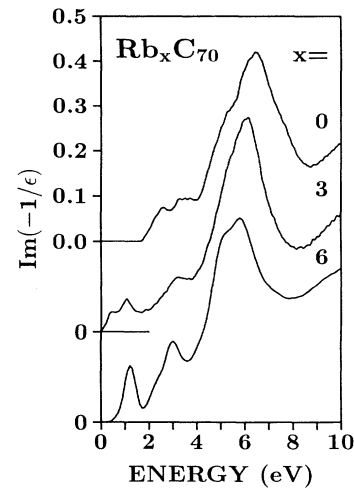


FIG. 5. The same as in Fig. 4 but for  $\text{Rb}_x\text{C}_{70}$  ( $x=0, 3,$  and  $6$ ).

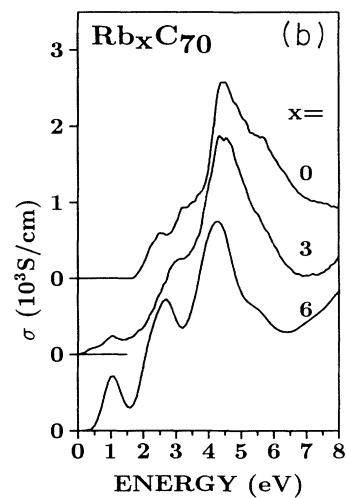
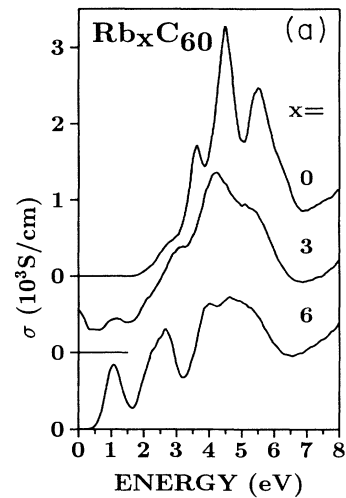


FIG. 6. Optical conductivities for (a)  $\text{Rb}_x\text{C}_{60}$  and (b)  $\text{Rb}_x\text{C}_{70}$  for  $x=0, 3,$  and  $6$ .

In Figs. 4 and 5 we show the low-energy range of the loss function ( $E < 10$  eV) for  $\text{Rb}_x\text{C}_{60}$  and  $\text{Rb}_x\text{C}_{70}$ , respectively, for  $x = 0, 3$ , and 6. In the undoped cases, a gap of about 2 eV is seen, followed by several maxima due to  $\pi$  plasmons caused by  $\pi \rightarrow \pi^*$  transitions. For  $x = 3$  new transitions appear in the gap. For  $x = 6$  a gap of about 0.5 eV opens again, which is consistent with the insulating properties of fully alkali-metal-doped fullerenes.

From the loss function, the function  $\text{Re}(1/\epsilon)$  can be derived via a Kramers-Kronig analysis. Subsequently, the real part of the dielectric function,  $\epsilon_1$ , and the imaginary part,  $\epsilon_2$ , can be calculated. Both are plotted in Figs. 2 and 3 for  $\text{Rb}_x\text{C}_{60}$  and  $\text{Rb}_x\text{C}_{70}$ , respectively, for dopant

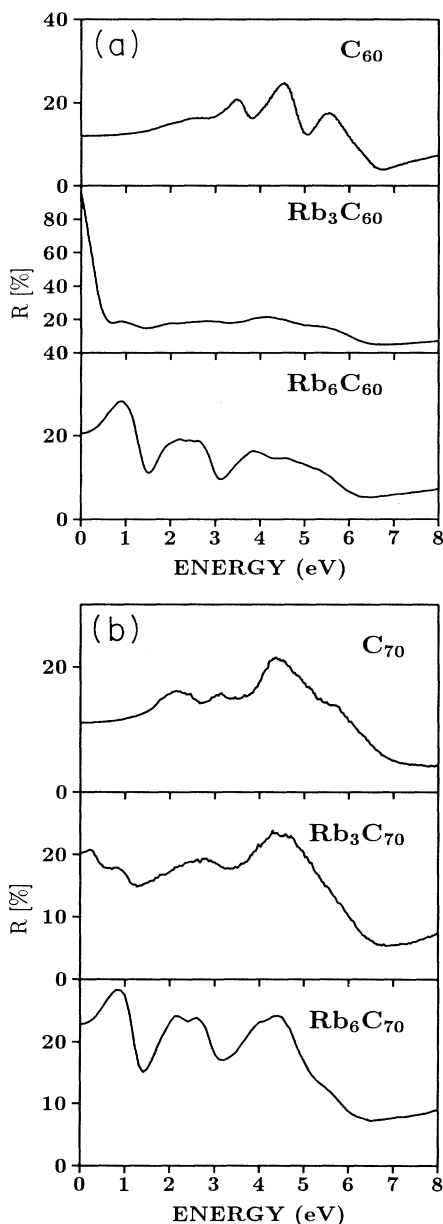


FIG. 7. Reflectivity curves for (a)  $\text{Rb}_x\text{C}_{60}$  and (b)  $\text{Rb}_x\text{C}_{70}$  for  $x = 0, 3$ , and 6.

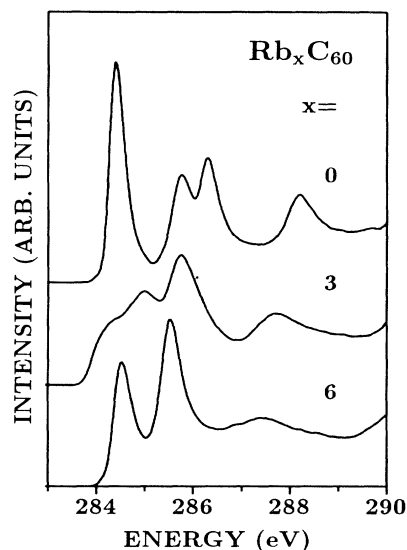


FIG. 8.  $\text{C}1s$ -absorption edges of  $\text{Rb}_x\text{C}_{60}$  for  $x = 0, 3$ , and 6.

concentrations  $x = 0, 3$ , and 6. In the  $\text{C}_{60}$  samples with  $x = 3$ , a large negative static dielectric constant  $\epsilon_1(0)$  is observed for small energies, as expected for a metallic solid. For  $\text{Rb}_3\text{C}_{70}$ ,  $\epsilon_1(0)$  does not clearly indicate a metallic behavior. For  $\text{Rb}_6\text{C}_{60}$  and  $\text{Rb}_6\text{C}_{70}$ ,  $\epsilon_1(0) = 7.1$  and  $\epsilon_1(0) = 8.0$ , respectively, are obtained. In all cases the imaginary part of the dielectric function  $\epsilon_2$ , shows  $\pi \rightarrow \pi^*$  intra and interband transitions for  $E < 8$  eV. Above 8 eV,  $\epsilon_2$  is dominated by  $\sigma \rightarrow \sigma^*$  transitions.

For comparison with available and future optical studies of undoped and doped  $\text{C}_{60}$  and  $\text{C}_{70}$ , in Figs. 6 and 7 we show the optical conductivities  $\sigma = \omega\epsilon_0\epsilon_2$  and the reflectivities, as calculated from the dielectric functions. The samples with  $x = 0$  and  $x = 6$  show optical conductivities and reflectivities typical of an insulator, while those for  $\text{Rb}_3\text{C}_{60}$  are typical of a metallic system. For  $\text{Rb}_3\text{C}_{70}$  the curves are more typical of an insulating system.

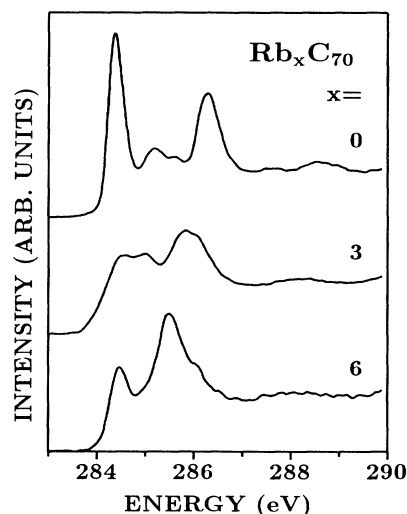


FIG. 9.  $\text{C}1s$ -absorption edges of  $\text{Rb}_x\text{C}_{70}$  for  $x = 0, 3$ , and 6.

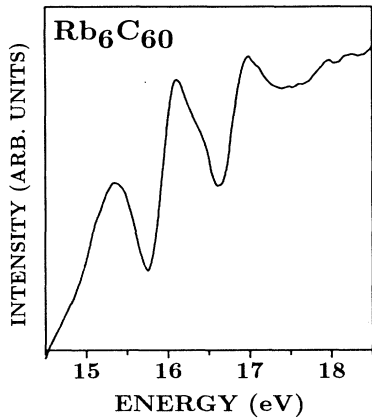


FIG. 10. Absorption edges of shallow core-level Rb4p electrons in  $Rb_6C_{60}$ .

In Figs. 8 and 9 we show C1s absorption edges for  $Rb_xC_{60}$  and  $Rb_xC_{70}$ , respectively, for  $x=0, 3$ , and 6. Below  $E \approx 290$  eV the maxima can be assigned to transitions from the C1s core level into  $\pi^*$  bands derived from unoccupied molecular orbitals. Above 290 eV (not shown) the spectral weight is dominated by  $1s \rightarrow \sigma^*$  transitions. Upon doping there is a considerable change of the spectra close to the threshold.

Finally, in Fig. 10 we show the loss function of  $Rb_6C_{60}$  in the energy range 14.5–18.5 eV for  $q=0$ . Transitions from Rb4p states into unoccupied states (probably mainly Rb4d states) are seen.

#### IV. DISCUSSION

##### A. $\pi + \sigma$ plasmon and $\sigma - \sigma^*$ transitions

The  $\pi + \sigma$  plasmon of undoped  $C_{60}$  and  $C_{70}$  has been discussed in some detail in a previous paper.<sup>19</sup> In common with graphite,<sup>47,48</sup> diamond,<sup>45</sup> amorphous carbon,<sup>45,49</sup> and conjugated polymers<sup>45,50</sup> this collective excitation of all valence electrons cannot be described in terms of the Drude model. In this model, plasmon energies of  $\hbar\omega_p = 21.6$  and 21.7 eV for  $C_{60}$  and  $C_{70}$ , respectively, are calculated from the Drude formula  $\omega_p^2 = 4\pi ne^2/m$  using the known atomic density and the fact that there are four valence electrons per carbon atom. Note that for  $q=0.15 \text{ \AA}^{-1}$ , the wavelength,  $\lambda$ , of these excitations is of the order of 40  $\text{\AA}$ , which is much larger than the diameter of the fullerene molecules. As pointed out previously,<sup>19</sup> the Lorentz model should be used to obtain the plasmon energy which gives  $\hbar\omega_p = (E_g^2 + 4\pi ne^2 \hbar^2/m)^{1/2}$ , where  $E_g$  is an average oscillator energy. In conjugated carbon compounds about  $\frac{3}{4}$  of the oscillator strength is determined by  $\sigma \rightarrow \sigma^*$  transitions which appear between 8 and  $\sim 35$  eV (see the  $\epsilon_2$  traces of Figs. 2 and 3). About  $\frac{1}{4}$  of the oscillator strength is determined by  $\pi \rightarrow \pi^*$  transitions in the energy range up to 8 eV. Since the oscillators have predominantly  $\sigma$  character we take the value  $E_g \sim 14$  eV from the fact that the  $\epsilon_2$  curves (see Sec. III) have a maximum at that energy. Then the plasmon energies for  $C_{60}$  and

$C_{70}$  are shifted from the Drude values to the Lorentz values  $\hbar\omega_p = 25.7$  and 25.8 eV, respectively, which are close to the experimental values. For the doped compounds, the additional valence and shallow core electrons (Rb4p) will shift the plasmon to higher energies. However, in the Rb-doped compounds the lattice constant is slightly increased, when compared with undoped fullerenes, and therefore the expected shift for the plasmon is almost completely compensated. This explains that experimentally no shift of the  $\pi + \sigma$  plasmon upon Rb doping has been detected.

Interesting features on the  $\pi + \sigma$  plasmon in graphite have been observed upon intercalation with alkali metals.<sup>51–53</sup> For stage-I compounds, these were strongest in  $KC_8$ , intermediate in  $RbC_8$ , and negligible in  $CsC_8$ . These features were explained in terms of atomic alkali-metal excitations also present in the alkali metals themselves and by  $\pi \rightarrow \pi^*$  transitions between backfolded bands due to the interaction with the wider lattice of alkali-metal atoms. No such structures can be seen in the loss functions shown in Figs. 1 and 2 for Rb-doped  $C_{60}$  and  $C_{70}$ . There are shoulders in the loss function of solid  $C_{60}$  at  $\sim 10$ ,  $\sim 13$ , and  $\sim 15$  eV which are, however, attributed to  $\sigma \rightarrow \sigma^*$  oscillators. In a first approximation these shoulders do not change upon doping with Rb. We have also studied other alkali-metal- (Li, Na, K, Cs) doped  $C_{60}$  films<sup>54</sup> and have also found that those compounds do not show features on the  $\pi + \sigma$  plasmon appearing upon doping. The atomic excitations responsible for these features should be almost as pronounced as in intercalated graphite, since the relative concentrations of alkali metals are similar. In fact, extremely small structures due to Rb4p shallow core electrons could be resolved between 15 and 17 eV as shown in Fig. 10. The three structures can be explained by the convolution of a Rb4p doublet with a Rb4d doublet both split by about 1 eV due to spin-orbit interaction. The reason why no features due to backfolded bands have been observed in any alkali-metal-doped fullerenes is that the alkali-metal sublattice has the same periodicity as that of the fullerene and that, contrary to graphite, which has wide bands, solid fullerenes have only narrow bands and therefore even backfolding were to occur, it would not change  $\pi - \pi^*$  transitions.

Regarding the  $\epsilon_2$  curve for  $C_{60}$  in Fig. 2, maxima appear at 10, 12, and 16 eV and  $\sim 22$  eV. From previous EELS investigations on conjugated carbon compounds<sup>45</sup> we know that these transitions can be mainly ascribed to  $\sigma \rightarrow \sigma^*$  transitions but mixed  $\pi \rightarrow \sigma^*$  and  $\sigma \rightarrow \pi^*$  transitions cannot be excluded. On doping with Rb the energy positions of these excitations do not change greatly. There is a tendency that with increasing  $x$  a broadening of the transitions leads to less pronounced structures in  $\epsilon_2$  in the energy range 8–35 eV. A similar tendency is found in the case of  $Rb_xC_{70}$  (see Fig. 3).

##### B. $\pi$ plasmon and $\pi \rightarrow \pi^*$ transitions (undoped fullerites)

For undoped  $C_{60}$ , a gap of about 2 eV is observed in the loss function (see Figs. 2 and 4), in  $\epsilon_2$  (see Fig. 2), and in the optical conductivity  $\sigma$  [see Fig. 6(a)]. At higher

energy several  $\pi \rightarrow \pi^*$  transitions appear in  $\epsilon_2$  and  $\sigma$ . These oscillators cause several maxima in the loss function. The sum of all  $\pi \rightarrow \pi^*$  oscillators leads to a minimum in the  $\epsilon_1$  curve close to 6 eV, which together with a low value of  $\epsilon_2$  at this energy causes a maximum at 6.5 eV in the loss function  $\text{Im}(-1/\epsilon) = \epsilon_2/(\epsilon_1^2 + \epsilon_2^2)$ . This maximum is commonly called a  $\pi$  plasmon because it is related to a collective oscillation of a sub group of valence electrons, namely the  $\pi$  electrons. The energy of the  $\pi$  plasmon in solid C<sub>60</sub> can be understood within a Lorentz model assuming  $E_g = 2$  eV and a background dielectric function  $\epsilon_\infty \sim 3$  due to  $\sigma$  electrons. In graphite<sup>47,48</sup> this  $\pi$  plasmon appears at 7 eV and is related to a strong  $\pi \rightarrow \pi^*$  transition at 4 eV. Similarly, in polyacetylene<sup>49</sup> there is only one  $\pi$  plasmon at 4.9 eV due to a  $\pi \rightarrow \pi^*$  transition across the fundamental gap at the zone boundary with an energy of 1.8 eV. The difference between the fullerenes and these conjugated carbon compounds is that the former are van der Waals bonded molecular crystals having many groups of narrow  $\pi$  bands leading to several well pronounced  $\pi \rightarrow \pi^*$  transitions, while in the graphite and polyacetylene there are wide  $\pi$  bands leading only to one pronounced optically allowed  $\pi \rightarrow \pi^*$  transition. Therefore, in the solid C<sub>60</sub> there are several additional well pronounced maxima in the loss function between 2 and 6.5 eV.

The onset of the spectral weight in the loss function, as well as in  $\epsilon_2$  and  $\sigma$ , is rather low in intensity. As mentioned in our previous EELS work on undoped fullerenes,<sup>19</sup> the reason for this is that the transition across the fundamental gap between the  $h_u$  and  $t_{1u}$  derived bands<sup>29</sup> is optically forbidden and for small values of momentum transfer,  $q$ , EELS measures dipole-allowed transitions. At higher momentum transfer, monopole and quadrupole transitions are allowed and therefore this  $h_u \rightarrow t_{1u}$  transition is strongly enhanced reaching a maximum at 2.2 eV for  $q \sim 0.9 \text{ \AA}^{-1}$ . Details of the intensity variation as a function of  $q$  will be reported elsewhere.<sup>54</sup> In agreement with our previous EELS work,<sup>19</sup> with optical measurements<sup>21</sup> and with calculations in the random phase approximation,<sup>35</sup> we assign the maxima in  $\sigma$  at 2.7, 3.6, 4.5, and 5.5 eV to optically allowed  $h_u \rightarrow t_{1g}$ ,  $(h_g, g_g) \rightarrow t_{1u}$ ,  $h_u \rightarrow h_g$ , and  $(h_g, g_g) \rightarrow t_{2u}$  transitions, respectively. We mentioned that at higher momentum transfer, some of the optically allowed transition become weaker and also at higher energies optically forbidden  $\pi \rightarrow \pi^*$  transitions appear.<sup>54</sup> The situation is similar to that in other molecular crystals (e.g.,  $\beta$  carotene), which show finite-size effects.<sup>55</sup>

In undoped C<sub>70</sub>, a  $\pi$  plasmon is also observed at 6.5 eV. On the other hand, the lower energy maxima in the loss function and the  $\pi \rightarrow \pi^*$  transition are much less pronounced than in C<sub>60</sub>. In the optical conductivity  $\sigma$ , shoulders are detected at 2.5, 3.2, and 5.7 eV and a maximum is seen at 4.4 eV. The gap is about 2 eV, as in C<sub>60</sub>. The reason for the broadening of the  $\pi \rightarrow \pi^*$  transitions in C<sub>70</sub> is the strongly reduced symmetry of this molecule in comparison to C<sub>60</sub>. This leads to a partial lifting of the high degeneracy of the molecular orbitals and so there are many more  $\pi \rightarrow \pi^*$  transitions which cannot be

resolved in the spectra. To the best of our knowledge there have been no published calculations of the optical properties of C<sub>70</sub>.

### C. $\pi$ electron excitations in Rb-doped fullerenes

In Rb<sub>3</sub>C<sub>60</sub> the gap seen in undoped C<sub>60</sub> is filled with new excitations of  $\pi$  valence electrons. In the loss function, two new maxima are observed at 0.5 and at 1.2 eV. Correspondingly, in the reflectivity an edge at 0.5 eV and a maximum at  $\sim 1$  eV is observed, while in the optical conductivity, a Drude-like decrease followed by a maximum at  $\sim 1.2$  eV is detected. At higher energies the  $\pi \rightarrow \pi^*$  transitions are slightly broadened and shifted to lower energies in comparison to the undoped fullerite. The new excitations can be explained in terms of a filling of the  $t_{1u}$  derived lowest group of three conduction bands by electrons from the dopant Rb5s orbitals. This has been detected previously in photoemission,<sup>12-16</sup> inverse photoemission,<sup>13,16</sup> x-ray-absorption,<sup>14</sup> and electron-energy-loss spectroscopy studies<sup>20</sup> of alkali-metal-doped C<sub>60</sub>. Calculation of the plasmon energy for the three conduction electrons per C<sub>60</sub> molecule in Rb<sub>3</sub>C<sub>60</sub> yields

$$\hbar\omega_p = (4\pi n e^2 \hbar^2 / m)^{1/2} = 2.3 \text{ eV}.$$

Subtracting the contributions from the Drude electrons in the  $\epsilon_1$  curve yields a background dielectric function due to  $\pi$  and  $\sigma$  electrons of  $\epsilon_\infty \sim 4.4$ . This would reduce the plasmon energy to  $\hbar\omega_p \sim 1.2$  eV. To obtain a value of  $\sim 0.5$  the effective mass of the electrons should be  $m^*/m \sim 4$ .

Using the known density of charge carries and the effective mass  $m^* = 4$  leads to a Fermi energy of  $\sim 0.25$  eV, which is close to what is derived from band-structure calculations giving a total width for the  $t_{1u}$ -derived half-filled band of about 0.5 eV. However, interband transitions may also shift the plasmon to lower energies. In the half-filled group of three conduction bands, interband transitions between the three bands are possible. Then, similarly as occurs in Ag (Ref. 56) the free-carrier plasmon is shifted close to the energy of interband transitions. Consequently, the maximum in the loss function of Rb<sub>3</sub>C<sub>60</sub> at 0.5 eV can be explained either by a charge-carrier plasmon of electrons with a high effective mass ( $m^*/m \sim 4$ ) or by an interband plasmon as in Ag. Of course, a combination of a high-effective mass and interband transitions could also shift the plasmon from 1.2 to 0.5 eV. In measurements of the optical reflectivity of K<sub>3</sub>C<sub>60</sub>,<sup>26</sup> a well defined plasmon edge has been observed at 0.73 eV, and similar values for  $\epsilon_\infty$  and  $m^*$  have been derived. In previous EELS studies on K<sub>3</sub>C<sub>60</sub>,<sup>20</sup> a plasmon has also been observed at 0.5 eV, however, it was less pronounced than in the present spectra of Rb<sub>3</sub>C<sub>60</sub>. This difference can be possibly explained by the fact that in the early studies of K<sub>3</sub>C<sub>60</sub>, the C<sub>60</sub> was contaminated with about 15% C<sub>70</sub>.

The plasmon width is  $\gamma \sim 0.4$  eV. This value is close to that detected in reflectivity data ( $\gamma = 0.31$  eV).<sup>26</sup> Assuming a simple Drude response, this corresponds to a scattering time of  $\tau = 1.6 \times 10^{-15}$  sec. We have also stud-

ied the dispersion of the plasmon at 0.5 eV. Within error bars no dispersion could be detected. This may be explained by the small Fermi energy of the conduction band electrons, since calculations in the random-phase approximation results in a dispersion coefficient being proportional to the Fermi energy.<sup>45</sup>

Regarding the optical conductivity data from  $\text{Rb}_3\text{C}_{60}$  at low energy, shown in Fig. 6(a), a dc conductivity  $\sigma(0) \sim 500$  S/cm is derived. This value is slightly larger than the dc conductivity values observed in Rb-doped  $\text{C}_{60}$  [ $\sigma(0) = 100$  S/cm].<sup>3</sup> The reason for this may be that for  $q = 0.15 \text{ \AA}^{-1}$  the wavelength of the plasmon is smaller than the dimensions of the grains ( $\sim 80 \text{ \AA}$ ). Therefore, grain-boundary effects do not appear in the dc conductivity measured by EELS.

A further peak at  $\sim 1.1$  eV is observed in the loss function of  $\text{Rb}_3\text{C}_{60}$ , which appears almost at the same energy in the trace of the optical conductivity shown in Fig. 6(a). This peak can be assigned to an interband transition between the half-filled  $t_{1u}$ -derived conduction bands and the  $t_{1g}$ -derived conduction bands. This assignment is consistent with the calculated optical properties of  $\text{K}_3\text{C}_{60}$  by Xu, Huang, and Ching.<sup>34</sup> This transition has also been detected in  $\text{K}_3\text{C}_{60}$  in the previous EELS studies,<sup>20</sup> absorption measurements,<sup>21</sup> and in the reflectivity data.<sup>26</sup>

In the fully doped compound,  $\text{Rb}_6\text{C}_{60}$ , the plasmon at 0.5 eV has disappeared because the  $t_{1u}$ -derived bands are now completely filled. This also causes an enhanced  $t_{1u} \rightarrow t_{1g}$  transition at  $\sim 1$  eV in the optical conductivity as more initial states are available. For this compound the low-energy data again agree quite well with the optical data calculated by Xu, Huang, and Ching.<sup>34</sup> The fact that our studies on other alkali-metal-doped compounds  $A_3\text{C}_{60}$  and  $A_6\text{C}_{60}$  ( $A = \text{Li, Na, K, and Cs}$ ) give very similar results to those from  $\text{Rb}_3\text{C}_{60}$  and  $\text{Rb}_6\text{C}_{60}$  indicate that the low-energy excitations of the  $\pi$  electron systems do not depend on the dopant ions and that the alkali-metal  $s$  electrons are fully transferred to the  $\text{C}_{60}$  molecules.

The results from  $\text{Rb}_3\text{C}_{70}$  are less clear. In common with  $\text{Rb}_3\text{C}_{60}$  there is a peak at 0.5 eV in the loss function followed by a stronger maximum at 1.2 eV. The first peak is much less pronounced in  $\text{Rb}_3\text{C}_{70}$  than in  $\text{Rb}_3\text{C}_{60}$ . The dc optical conductivity for  $\text{Rb}_3\text{C}_{70}$  is zero and the reflectivity is only 20%. Both these properties would indicate insulating behavior. However, we should mention that the quasielastic peak, which we have subtracted from the measurements, extends up to 0.3 eV and therefore the measurements below this energy are less reliable. Consequently, our measurements cannot exclude a finite optical conductivity at energies below  $\sim 0.3$  eV and the system may be metallic at low energies. On the other hand, our measurements clearly show a strongly reduced optical conductivity for  $\text{Rb}_3\text{C}_{70}$  below  $\sim 0.5$  eV when compared with  $\text{Rb}_3\text{C}_{60}$ . This is in line with the measurements of the dc conductivity of these compounds.<sup>3</sup> The reasons for this reduced optical ( $E < 0.3$  eV) and dc conductivities in  $\text{Rb}_3\text{C}_{70}$  may be the lower symmetry of the  $\text{C}_{70}$  molecule, which lifts the high degeneracy of the molecular orbitals observed in  $\text{C}_{60}$ . This can lead to

broader conduction bands which for a certain filling may give a small or zero density of states at the Fermi level. This may also be the reason for the fact that superconductivity has not been observed for  $\text{Rb}_3\text{C}_{70}$ .

The optical conductivity of  $\text{Rb}_3\text{C}_{60}$  and  $\text{Rb}_3\text{C}_{70}$  in the energy range 0.7–5 eV are very similar. This also holds for  $\text{Rb}_6\text{C}_{60}$  and  $\text{Rb}_6\text{C}_{70}$ , where the transitions at 1 eV are quantitatively the same, while the intensity of the transitions at 2.7,  $\sim 4$ , and  $\sim 4.8$  eV differs slightly. In analogy to  $\text{Rb}_6\text{C}_{60}$ , the 1 eV transition in  $\text{Rb}_6\text{C}_{70}$  can probably be assigned to a transition from the lowest unoccupied molecular orbital (LUMO) derived occupied conduction bands to the LUMO+1-derived unoccupied conduction bands.

#### D. C1s absorption edges

The C1s absorption edges of  $\text{Rb}_x\text{C}_{60}$  are very similar to those published previously of  $\text{K}_x\text{C}_{60}$ .<sup>14,20</sup> Similar results have also been obtained for  $A_x\text{C}_{60}$  ( $A = \text{Li, Na, and Cs}$ ).<sup>54</sup> This indicates once more that the electronic structure of the alkali fullerides is independent of the counterions except for the differences in lattice constants leading to a variation of the density of states at the Fermi level. The four peaks in the C1s absorption edge for undoped  $\text{C}_{60}$  correspond to transitions from the  $1s$  level into groups of unoccupied  $\pi^*$  bands. Upon doping with Rb, there are more valence electrons on the C atoms which screen the nuclear potential and therefore reduce the binding energy of the  $1s$  level. Thus, with increasing  $x$ , the spectra are shifted to lower energies. In addition, for  $x = 3$  the lowest peak is reduced by a factor of about 2 indicating a half-filled LUMO-derived band. Correspondingly, for  $x = 6$  this lowest peak has completely disappeared, which directly shows the complete filling of the lowest group of conduction bands. Moreover, the doping dependent changes in the energy differences between the  $1s \rightarrow \pi^*$  transitions indicate a nonrigid-band behavior of the  $\text{Rb}_x\text{C}_{60}$  system. Although the energy differences and the widths of the  $\pi^*$  bands and the  $1s \rightarrow \pi^*$  transitions matrix elements are different between  $\text{C}_{60}$  and  $\text{C}_{70}$ , the shift of the spectra to lower energy with increasing  $x$  and the filling of the LUMO-derived bands are also observed for  $\text{Rb}_x\text{C}_{70}$ .

#### V. SUMMARY

The partial filling of the lowest group of conduction bands has been observed for  $\text{Rb}_3\text{C}_{60}$  and  $\text{Rb}_3\text{C}_{70}$ . The optical conductivity at low energies ( $E < 0.5$  eV) is considerably smaller (or zero) for  $\text{Rb}_3\text{C}_{70}$  when compared with  $\text{Rb}_3\text{C}_{60}$ . This may explain the nonobservation of superconductivity in  $\text{Rb}_3\text{C}_{70}$ . The low-energy excitation spectra of  $\text{Rb}_6\text{C}_{60}$  and  $\text{Rb}_6\text{C}_{70}$  are very similar indicating in both cases a complete filling of the lowest group of conduction bands. The present investigations show a nonrigid-band behavior for the  $\pi$ -electron system in  $\text{Rb}_x\text{C}_{60}$  and  $\text{Rb}_x\text{C}_{70}$ . The  $\sigma$ -electron system appears to be unchanged upon doping with Rb. Up to now no

differences in the  $\pi$  electronic structure have been observed for replacing Rb by other alkali-metal ions. This clearly shows that the alkali  $s$  electrons are completely transferred to the fullerene molecules and that the hybridization between the levels of the fullerene molecules and those of alkali-metal ions is small.

#### ACKNOWLEDGMENTS

We thank P. Adelman for support during production of fullerenes and A. Masaki for preparation of some of the fullerite films. Critical reading of the manuscript by M. S. Golden is acknowledged.

- <sup>1</sup>H. W. Kroto, J. R. Heath, S. C. O'Brian, R. F. Curl, and R. E. Smalley, *Nature (London)* **318**, 162 (1985).
- <sup>2</sup>W. Krätschmer, L. D. Lamb, K. Fostiropoulos, and D. R. Huffman, *Nature (London)* **347**, 354 (1990).
- <sup>3</sup>R. C. Haddon, A. F. Hebard, M. J. Rosseinsky, D. W. Murphy, S. J. Duclos, K. B. Lyons, B. Miller, J. M. Rosamilia, R. M. Fleming, A. R. Kortan, S. H. Glarum, A. V. Makhija, A. J. Muller, R. H. Eick, S. M. Zahurak, R. Tycko, G. Dabaghi, and F. A. Thiel, *Nature (London)* **350**, 320 (1991).
- <sup>4</sup>A. F. Hebard, M. J. Rosseinsky, R. C. Haddon, D. W. Murphy, S. H. Glarum, T. T. M. Palstra, A. P. Ramirez, and A. R. Kortan, *Nature (London)* **350**, 600 (1991).
- <sup>5</sup>K. Tanigaki, T. W. Ebbesen, S. Saito, J. Mizuki, J. S. Tsai, Y. Kubo, and S. Kuroshima, *Nature (London)* **352**, 222 (1991).
- <sup>6</sup>A. A. Zakhidov, K. Imaeda, A. Ugawa, K. Yakushi, H. Inokuchi, Z. Iqbal, R. H. Baughman, B. L. Ramakrishna, and Y. Achiba, *Physica C* **185–189**, 411 (1991).
- <sup>7</sup>C. M. Varma, J. Zaanen, and K. Raghavachari, *Science* **254**, 989 (1991).
- <sup>8</sup>M. Schlüter, M. Lannoo, M. Needels, G. A. Baraff, and D. Tomanek, *Phys. Rev. Lett.* **68**, 526 (1992).
- <sup>9</sup>I. I. Mazin, S. N. Rashkeev, V. P. Antropov, O. Jepsen, A. I. Liechtenstein, and O. K. Andersen, *Phys. Rev. B* **45**, 5114 (1992).
- <sup>10</sup>F. C. Zhang, M. Ogata, and T. M. Rice, *Phys. Rev. Lett.* **67**, 3452 (1991).
- <sup>11</sup>S. Chakravarty, M. P. Gelfand, and S. Kivelson, *Science* **254**, 970 (1991).
- <sup>12</sup>J. H. Weaver, J. L. Martins, T. Komeda, Y. Chen, T. R. Ohno, G. H. Kroll, N. Troullier, R. E. Haufler, and R. E. Smalley, *Phys. Rev. Lett.* **66**, 1741 (1991).
- <sup>13</sup>P. J. Benning, J. L. Martins, J. H. Weaver, L. P. F. Chibante, and R. E. Smalley, *Science* **252**, 1417 (1991).
- <sup>14</sup>C. T. Chen, L. H. Tjeng, P. Rudolf, G. Meigs, J. E. Rowe, J. Chen, J. P. McCauley, Jr., A. B. Smith III, A. R. McGhie, W. J. Romanow, and E. W. Plummer, *Nature (London)* **352**, 603 (1991).
- <sup>15</sup>G. K. Wertheim, J. E. Rowe, D. N. E. Buchanan, E. E. Chaban, A. F. Hebard, A. R. Kortan, A. V. Makhija, and R. C. Haddon, *Science* **252**, 1419 (1991).
- <sup>16</sup>T. Takahashi, S. Suzuki, T. Morikawa, H. Katayama-Yoshida, S. Hasegawa, H. Inokuchi, K. Seki, K. Kikuchi, S. Suzuki, K. Ikemoto, and Y. Achiba, *Phys. Rev. Lett.* **68**, 1232 (1992).
- <sup>17</sup>M. Merkel, M. Knupfer, M. S. Golden, J. Fink, R. Seemann, and R. L. Johnson, *Phys. Rev. B* **47**, 11 470 (1993).
- <sup>18</sup>L. J. Terminello, D. K. Shuh, F. J. Himpsel, D. A. Lapiano-Smith, J. Stöhr, D. S. Bethune, and G. Meijer, *Chem. Phys. Lett.* **182**, 491 (1991).
- <sup>19</sup>E. Sohmen, J. Fink, and W. Krätschmer, *Z. Phys. B* **86**, 87 (1992).
- <sup>20</sup>E. Sohmen, J. Fink, and W. Krätschmer, *Europhys. Lett.* **17**, 51 (1992).
- <sup>21</sup>T. Pichler, M. Matus, J. Kürti, and H. Kuzmany, *Solid State Commun.* **81**, 859 (1992).
- <sup>22</sup>S. L. Ren, Y. Wang, A. M. Rao, E. McRae, J. M. Holden, T. Hager, K.-A. Wang, W.-T. Lee, H. F. Ni, J. Selegue, and P. C. Eklund, *Appl. Phys. Lett.* **59**, 2678 (1991).
- <sup>23</sup>K. Wang, Y. Wang, P. Zhou, J. M. Holden, S. Ren, G. T. Hager, H. F. Ni, P. C. Eklund, G. Dresselhaus, and M. Dresselhaus, *Phys. Rev. B* **45**, 1955 (1992).
- <sup>24</sup>Y. Wang, J. M. Holden, A. M. Rao, W. Lee, X. X. Bi, S. L. Ren, G. W. Lehman, G. T. Hager, and P. C. Eklund, *Phys. Rev. B* **45**, 14 396 (1992).
- <sup>25</sup>M. K. Kelly, P. Etchegoin, D. Fuchs, W. Krätschmer, and K. Fostiropoulos, *Phys. Rev. B* **46**, 4963 (1992).
- <sup>26</sup>Y. Iwasa, K. Tanaka, T. Yasuda, T. Koda, and S. Koda, *Phys. Rev. Lett.* **69**, 2284 (1992).
- <sup>27</sup>G. Gensterblum, J. J. Pireaux, P. A. Thiry, R. Caudano, J. P. Vigneron, Ph. Lambin, and A. A. Lucas, *Phys. Rev. Lett.* **67**, 2171 (1991).
- <sup>28</sup>A. Lucas, G. Gensterblum, J. J. Pireaux, P. A. Thiry, R. Caudano, J. P. Vigneron, Ph. Lambin, and W. Krätschmer, *Phys. Rev. B* **45**, 13 694 (1992).
- <sup>29</sup>S. Saito and A. Oshiyama, *Phys. Rev. Lett.* **66**, 2637 (1991).
- <sup>30</sup>S. Satpathy, V. P. Antropov, O. K. Andersen, O. Jepsen, O. Gunnarsson, and A. J. Liechtenstein, *Phys. Rev. B* **46**, 1773 (1992).
- <sup>31</sup>D. L. Novikov, V. A. Gubanov, and A. J. Freeman, *Physica C* **191**, 399 (1992).
- <sup>32</sup>S. C. Erwin and W. E. Pickett, *Science* **254**, 842 (1991).
- <sup>33</sup>W. Y. Ching, M.-Z. Huang, Y.-N. Xu, W. G. Harter, and F. T. Chan, *Phys. Rev. Lett.* **67**, 2045 (1991).
- <sup>34</sup>Y.-N. Xu, M.-Z. Huang, and W. Y. Ching, *Phys. Rev. B* **44**, 13 171 (1991).
- <sup>35</sup>G. F. Bertsch, A. Bulgac, D. Tománek, and Y. Wang, *Phys. Rev. Lett.* **67**, 2690 (1991).
- <sup>36</sup>R. W. Lof, M. A. van Veenendaal, B. Koopmans, H. T. Jonkman, and G. A. Sawatzky, *Phys. Rev. Lett.* **68**, 3924 (1992).
- <sup>37</sup>V. P. Antropov, O. Gunnarsson, and O. Jepsen, *Phys. Rev. B* **46**, 13 647 (1992).
- <sup>38</sup>J. Fink, E. Sohmen, and W. Krätschmer, in *Electronic Properties and Mechanisms of High-T<sub>c</sub> Superconductors*, edited by T. Oguchi, K. Kadowaki, and T. Sasaki (North-Holland, Amsterdam, 1992), p. 81.
- <sup>39</sup>P. W. Stephens, L. Mihaly, P. Lee, R. L. Whetten, S.-M. Huang, R. B. Kaner, F. Diederich, and K. Holczer, *Nature (London)* **351**, 632 (1991).
- <sup>40</sup>O. Zhou, J. E. Fischer, N. Coustel, S. Kycia, Q. Zuh, A. R. McGhie, W. J. Romanow, J. P. McCauley, Jr., A. B. Smith III, and D. E. Cox, *Nature (London)* **351**, 462 (1991).
- <sup>41</sup>R. M. Fleming, A. P. Ramirez, M. J. Rosseinsky, D. W. Murphy, R. C. Haddon, S. M. Zahurak, and A. V. Makhija, *Nature (London)* **352**, 701 (1991).
- <sup>42</sup>P. W. Stephens, L. Mihaly, J. B. Wiley, S. Huang, R. B. Kaner, F. Diederich, R. L. Whetten, and K. Holczer, *Phys.*

- Rev. B **45**, 543 (1992).
- <sup>43</sup>Q. Zhu, O. Zhou, N. Coustel, G. B. M. Vaughan, J. P. McCauley, Jr., W. J. Romanow, J. E. Fischer, and A. B. Smith III, *Science* **254**, 545 (1991).
- <sup>44</sup>M. J. Rosseinsky, A. P. Ramirez, S. H. Glarum, D. W. Murphy, R. C. Haddon, A. F. Hebard, T. T. M. Palstra, A. R. Kortan, S. M. Zahurak, and A. V. Makhija, *Phys. Lett.* **66**, 2830 (1991).
- <sup>45</sup>J. Fink, *Adv. Electron. Electron. Phys.* **75**, 121 (1989).
- <sup>46</sup>P. Livins, T. Aton, and S. E. Schnatterly, *Phys. Rev. B* **38**, 5511 (1988).
- <sup>47</sup>K. Zeppenfeld, *Z. Phys.* **243**, 229 (1971).
- <sup>48</sup>U. Büchner, *Phys. Status Solidi B* **81**, 227 (1977).
- <sup>49</sup>J. Fink, Th. Müller-Heinzerling, J. Pflüger, B. Scheerer, B. Dischler, P. Koidl, A. Bubenzer, and R. E. Sah, *Phys. Rev. B* **30**, 4713 (1984).
- <sup>50</sup>J. Fink and G. Leising, *Phys. Rev. B* **34**, 5320 (1986).
- <sup>51</sup>J. J. Ritsko, E. J. Mele, and I. P. Gates, *Phys. Rev. B* **24**, 6114 (1981).
- <sup>52</sup>L. A. Grunes and J. J. Ritsko, *Phys. Rev. B* **28**, 3439 (1983).
- <sup>53</sup>M. E. Preil, L. A. Grunes, J. J. Ritsko, and J. E. Fischer, *Phys. Rev. B* **30**, 5852 (1984).
- <sup>54</sup>H. Romberg *et al.* (unpublished).
- <sup>55</sup>E. Pellegrin, J. Fink, and S. L. Dreschler, *Phys. Rev. Lett.* **66**, 2022 (1991).
- <sup>56</sup>H. Ehrenreich, H. R. Phillipp, and B. Segall, *Phys. Rev.* **132**, 1918 (1963).